Aerosol and Air Quality Research, 18: 1019–1031, 2018

ISSN: 1680-8584 print / 2071-1409 online
doi: 10.4209/aaqr.2018.01.0038

Variation of Atmospheric PAHs in Northern Taiwan during Winter and Summer Seasons

Nguyen-Duy Dat, Jia-Ming Lyu, Moo-Been Chang*

Graduate Institute of Environmental Engineering, National Central University, Taoyuan 32001, Taiwan

ABSTRACT

Ambient air samples were collected simultaneously at three sites in winter and summer to investigate the characteristic variations of PAHs in northern Taiwan. In winter, the highest concentration was observed at urban site (225 ± 25.0 ng m^{-3}), followed by industrial and rural sites (173 ± 28.7 and 148 ± 12.9 ng m^{-3}, respectively). However, in summer, the highest PAHs concentration was measured at rural site (230 ± 8.0 ng m^{-3}), followed by urban and industrial sites (205 ± 29.2 and 200 ± 44.1 ng m^{-3}, respectively). Based on the air mass back trajectory, the air mass passing through more PAH sources before reaching the sampling site is the reason for higher PAH level being measured at rural site in summer. The highest BaP-TEQ concentration measured at rural site in summer suggests that human exposure to PAHs in summer should receive more attention. Based on the diagnostic ratios, samples collected at industrial site in two seasons are closely related to combustions of solid fuel and petroleum. At rural and urban sites, PAHs measured in winter are influenced by mixed sources of solid fuel/petroleum combustions and petroleum evaporation, while the sources of PAHs are more related to petroleum evaporation in summer. The gas/particle partitioning coefficients (K_p) correlated well with the sub-cooled liquid vapor pressures (P^o_L) of PAHs with the slopes higher than –1 (the r^2 ranging from 0.835 to 0.909). The slope values indicate that both adsorption and absorption might govern gas/particle partitioning of PAHs. Comparison between different models reveals that adsorption of soot carbon is the major mechanism governing gas/particle partitioning.

Keywords: Junge-Pankow model; Absorption K_{OA} model; Soot-air model; PAHs concentration; Distribution.

INTRODUCTION

Polycyclic aromatic hydrocarbons (PAHs) are a group of organic compounds composed of multiple aromatic rings, which are mainly formed during incomplete combustion and pyrolysis of materials containing carbon and hydrogen, such as coal, oil, wood and petroleum products (Ravindra *et al.*, 2008). PAHs are environmentally persistent with varying structures and toxicity and are well recognized as carcinogenic, teratogenic and genotoxic compounds (Yang *et al.*, 2010a). Therefore, investigating the occurrence of atmospheric PAHs is important for reducing human exposure to these toxic pollutants.

Characteristics of atmospheric PAHs depend on the sources and meteorological parameters, including wind speed/direction, temperature, rainfall and sunshine duration (Dat and Chang, 2017). Higher atmospheric PAHs concentrations are primarily found at locations with higher PAHs emission, for instance, higher PAHs concentrations are reported in industrial, urban or residential regions compared with those measured in remote or rural areas (Callen *et al.*, 2011; Anastasopoulos *et al.*, 2012; Brown and Brown, 2012; Xia *et al.*, 2013; Garrido *et al.*, 2014; Liu *et al.*, 2014). Concentration of particulate PAHs during sugarcane-burning period is about 10 times higher than that in non-sugarcane-burning period as reported by Cristale *et al.* (2012). Significant correlation between population density and atmospheric PAH concentration was observed by Hafner *et al.* (2005). However, higher atmospheric PAHs level was found in rural village if compared with urban site due to greater use of domestic coal and biofuel burning in rural village (Wang *et al.*, 2011). Higher levels of ambient PAHs were observed in wintertime compared to those measured in other seasons (Cincinelli *et al.*, 2007; Liu *et al.*, 2008; Van Drooge *et al.*, 2010; Wang *et al.*, 2011; Dvorská *et al.*, 2012; Masih *et al.*, 2012; Xia *et al.*, 2013; Lv *et al.*, 2016; Tomaz *et al.*, 2016; Wang *et al.*, 2016). Higher wind speed would reduce the PAH level by increasing dilution and dispersion of pollutants, and a negative correlation between PAH concentration and wind speed was observed (Tan *et al.*, 2006; Sharma *et al.*, 2007). Masih *et al.* (2012) found that PAH concentration decreases with the increase of temperature and wind speed. Elorduy *et al.* (2016) also indicated that temperature, wind speed, and atmospheric

*Corresponding author.
Tel.: +886-3-4227151, ext. 34663, Fax: +886-3-4226774
E-mail address: mbchang@ncuen.ncu.edu.tw

pressure are the significant meteorological parameters influencing PAH concentration.

Atmospheric PAHs are found in both gaseous and particulate phases. In general, gas-phase PAHs predominate as reported by various studies (Akyüz and Çabuk, 2010; Yang *et al.*, 2010b; Gregoris *et al.*, 2014, Wu *et al.*, 2014; Lai *et al.*, 2017). Light-molecular-weight (LMW) PAHs (2- to 3-ring) dominate in gas phase due to their higher vapor pressures, and high-molecular-weight (HMW) PAHs (5, 6-ring) with low vapor pressures are main contributors in particle phase, while medium-molecular-weight (MMW) PAHs (4-ring) associate with both gas and particulate phases (Cheruyiot *et al.*, 2015; Dat and Chang, 2017). After being released from the sources into atmosphere, gas/particle partitioning of PAHs affects their transport, degradation, deposition and subsequent fate in the environment (Lv *et al.*, 2016). This partition behavior also affects the level of human exposure to PAHs; therefore, investigating the gas/particle partitioning of PAHs would provide useful information on the transport, fate and effect of PAHs to human health. Distribution of a semi-volatile organic compound (SVOC) between gaseous and particulate phases is usually evaluated by gas/particle partitioning coefficient, as shown in Eq.(1), where C_p and C_g are particulate- and gaseous-phase concentration (ng m^{-3}), respectively and TSP is the total suspended particle concentration (μg m^{-3}). The definition of K_p reveals that a compound with a larger K_p value is of higher tendency to associate with particulate matter. However, K_p value itself does not reveal any information regarding the nature of partitioning process. Generally, gas/particle partitioning of SVOC or PAHs can be governed by adsorption onto surface, absorption into the organic matter (OM) of aerosol or the combination of adsorption and absorption (Pankow, 1994). For better description of possible mechanisms governing gas/particle partitioning of PAHs, some models were developed. Junge-Pankow model (Yamasaki *et al.*, 1982; Pankow, 1994) and K_{OA} absorption model (Finzio *et al.*, 1997; Harner and Bidleman, 1998) are developed with the assumption of physical adsorption onto particle surface and absorption into the organic matter of aerosol as the main mechanisms of two models, respectively. Dachs and Eisenreich (2000) indicated that soot plays a major role on gas/particle partitioning of PAHs. In order to include the role of soot into the calculation of gas/particle partitioning, Dachs and Eisenreich (2000) established a soot-air partition coefficient (K_{SA}) and proposed a method for the evaluation of both roles played by adsorption onto soot and absorption into organic matter. Pankow and Bidleman (1992) reported that well correlation between the observed log of gas/particle partitioning coefficient ($\log K_p$) and log of the PAH sub-cooled liquid vapor pressure ($\log P^0_L$) according to Eq. (2), and the slope values are usually close to –1, which corresponds to adsorption mechanism. Pankow (1994) indicates that Eq. (2) is also linearly correlated if absorption is the dominant mechanism, which reveals that regardless of the importance of adsorbent or absorbent in gas/particle partitioning, the plot of $\log K_p$ vs $\log P^0_L$ should be correlated with the slope close to –1. Goss and Schwarzenbach (1998) reviewed the slope m_r for field data of gas/particle partitioning from literature and indicated that under equilibrium conditions, the slope m_r should be equal to –1 if either adsorption or absorption mechanism governs the gas/particle PAH partitioning. The slope significantly steeper than –1 reveals the adsorption on a strong adsorbent and slope shallower than –0.6 suggests the absorption into an absorbent with high cohesive energy. On the other hand, the slope in the range of –0.6 to –1 occurs when either absorption or adsorption is involved. Nowadays, this result is used as the most popular criterion to evaluate the mechanism governing gas/particle partitioning of PAHs (Dat and Chang, 2017). The major mechanism governing the gas/particle partitioning of PAHs can be identified by using the $\log K_p$-$\log P^0_L$ relationship and comparing the fitting of three different models including Junge-Pankow model, absorption K_{OA} model and soot-air model.

$$K_p = (C_p/TSP)/C_g \quad (1)$$

$$\log K_p = m_r \log P^0_L + b_r \quad (2)$$

Although some studies on PAHs occurrences in Taiwan have been conducted (Chen *et al.*, 2009; Chen *et al.*, 2016; Lai *et al.*, 2017; Yang *et al.*, 2017), investigation on atmospheric PAHs has not been reported in northern Taiwan where some big cities with high density of population and industrial parks are located. Taoyuan City, a highly industrialized and densely populated city located in northern Taiwan, has the high potential risk of PAHs. Investigating the concentrations, distributions, sources and gas/particle partitioning of atmospheric PAHs collected in different sites in winter and summer would provide the information for better understanding the PAH characteristics and human risk associated with PAHs in this area. In this study, the samples were collected simultaneously at three different sites representing urban, rural and industrial characteristics in winter time and summer time.

MATERIALS AND METHODS

Sampling

In order to investigate the characteristics of PAHs in different areas located in Taoyuan City, ambient air samples were simultaneously collected at 3 sites, including a rural site (roof top of a 4-story building located in NCU campus), an urban site (roof top of a 5-story building in a high school campus located in Zhongli District) and an industrial site (roof top of a 2-story office in an Kuanyin industrial park). The distances between rural and industrial sites, rural and urban sites are 15.5 and 4.5 km, respectively. The locations of sampling sites are presented in Fig. 1.

Two samples in winter time (20–24th February 2017) and three samples in summer time (24th July–1st August 2017) were collected at each site with Sibata high-volume air samplers at a sampling rate of 500 L min^{-1}. Each sample was collected for 2 days with the total volume of 1440 m^3. Gas-phase PAHs were adsorbed by a sandwich cartridge of PUF/XAD-2/PUF containing 30 g XAD-2 and a TE-1123-4

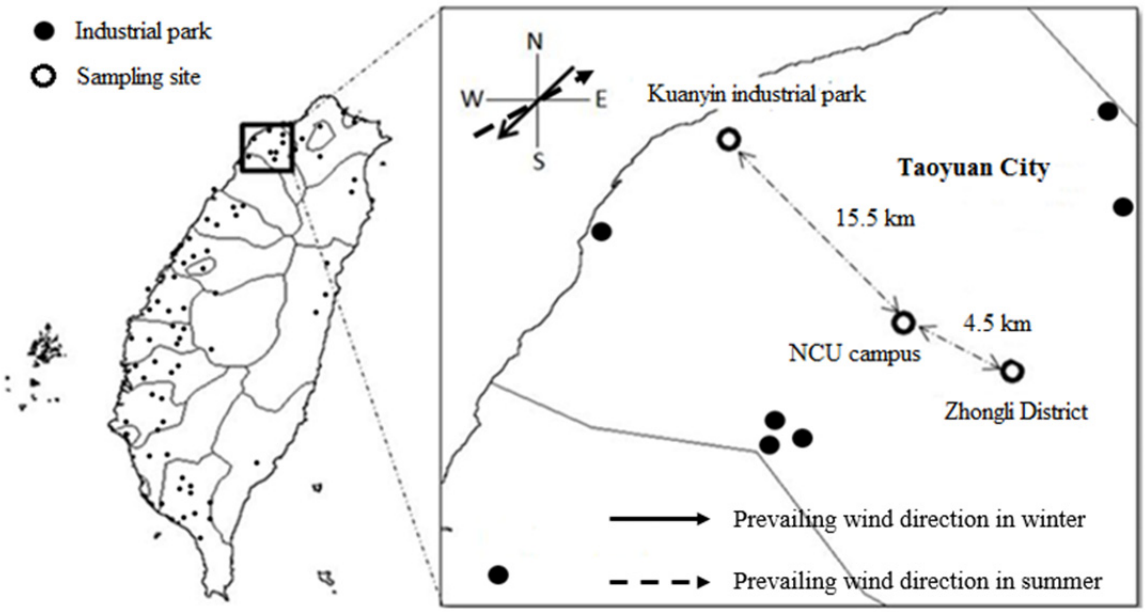

Fig. 1. Locations of sampling sites.

PUF (3 inch long, Tisch Environmental), while particulate-phase PAHs were collected by quartz fiber filter (QFF, Advantec, Japan). Prior to sampling, XAD-2 and PUF were pre-cleaned in Soxhlet extractor with toluene for 24 hrs and were dried by a nitrogen gas stream at 50°C in a vacuum oven to remove toluene, while the filters were baked at 900°C for 4 hrs to remove any traces of organics and weighed at ambient temperature. Fluorene-D10 and p-Terphenyl-D14 are added into the sandwich cartridges as surrogate standards before sampling. After sampling, QFF and sandwich cartridge were separately wrapped in aluminum foil and stored at < 5°C until analysis.

Meteorological parameters including ambient temperature, relative humidity (RH), wind speed, wind direction and rainfall were recorded at each sampling site. The levels of criteria pollutants including (SO_2, NO_x, CO, O_3, PM) were downloaded from Taiwan EPA website. Air mass origins were determined using the HYSPLIT transport and dispersion model from the NOAA Air Resources Laboratory. The 48-hour back trajectory was used to identify the air mass origins for each sampling event.

Analysis

Samples were extracted for 24 hours by Soxhlet extraction with dichloromethane (DCM). All samples was added an isotope-spiked solution of PAHs (Wellington Laboratories Inc.) before extraction to quantify the concentration of each PAH congener. The DCM extract was then concentrated to approximately 10 mL by rotary evaporation. DCM was replaced with hexane by three times of adding 60 ml of hexane and concentrating to remove completely DCM. The sample was then passed through a clean-up column that was packed with 10 g of activated silica gel and 1 g Na_2SO_4. The column was eluted by hexane and DCM to obtain PAHs in the purifying solution and then, the extract was condensed to 2 mL by rotary evaporation. The collected eluent was reconcentrated to approximately 500 μL, with a gentle nitrogen stream and was added recovery standards before analysis. Sixteen USEPA-priority PAHs including naphthalene (NAP), acenaphthylene (ACY), acenaphthene (ACE), fluorene (FLO), phenanthrene (PHE), anthracene (ANT), fluoranthene (FLA), pyrene (PYR), benz[a]anthracene (BaA), chrysene (CHR), benzo[b]fluoranthene (BbF), benzo[k]fluoranthene (BkF), benzo[a]pyrene (BaP), dibenz[a,h]anthracene (DahA), benzo [g,h,i]perylene (BghiP) and indeno[1,2,3-cd]pyrene (IcdP) were analyzed by GCMS (Agilent 6890-5973N) using a fused silica capillary column DB-5 MS (60 m × 0.25 mm × 0.25 m) under positive EI conditions, and data were obtained in the selected ion monitoring (SIM) mode.

Quality Control

Field blanks and method blanks were extracted and analyzed in the same way as field samples. Only low contents of NAP and PHE were detected in the PUF/XAD-2/PUFs of field blank samples (< 0.5 μg and < 5 × 10^{-3} μg per cartridge, respectively). The recoveries of internal standards range from 85 to 105%, except for NAP (60–75%). The average recoveries of surrogate standards are 95% and 82% for Fluorene-D10 and p-Terphenyl-D14, respectively. The MDLs range from 2.01 × 10^{-3} ng m^{-3} for PYR to 10.0 × 10^{-3} ng m^{-3} for IcdP.

RESULTS AND DISCUSSION

Atmospheric Concentrations

Meteorological parameters including wind speed, temperature, relative humidity (RH), rainfall and TSP concentration corresponding to different samples collected at three sites in the winter and summer time are presented in Table S1. Generally, wind speed, relative humidity and rainfall in winter are higher than those in summer. Wind

speed and TSP concentration measured at the industrial site are higher than those measured at two other sites in both winter and summer. The average TSP concentrations measured at industrial site in summer is 215 ± 76.2 μg m^{-3}, which is significantly higher than that in winter (103 ± 16.8 μg m^{-3}). However, the reverse trends are observed for both urban and rural sites in which the TSP concentrations in winter (57.4 ± 16.0 and 51.9 ± 16.8 μg m^{-3}, respectively) are higher than those in summer (36.8 ± 1.60 and 43.0 ± 1.20 μg m^{-3}, respectively).

The average mass and BaP-TEQ concentrations of atmospheric PAHs in the winter and the summer at three sites are presented in Fig. 2. In term of average annual concentration, the highest concentration was found at urban site (213 ± 23.3 ng m^{-3}), followed by rural site (197 ± 41.7 ng m^{-3}) and industrial site (189 ± 41.0 ng m^{-3}). In the winter, the highest concentration was observed at urban site (200–250 ng m^{-3}), followed by industrial site (201–144 ng m^{-3}) and rural site (135–161 ng m^{-3}). However, in summer, the PAHs concentration measured at rural site was the highest (219–237 ng m^{-3}), followed by urban site (170–246 ng m^{-3}) and industrial site (140–244 ng m^{-3}). Compared with previous studies, the PAH concentrations obtained in this study are lower than those reported in North China Plain by Wang *et al.* (2011) for urban and rural sites (∑15PAHs = 89.8–1616 ng m^{-3}, sampling time: 2007–2008). However, the PAH concentrations at urban and rural sites measured in this study are higher those reported by Anastasopoulos *et al.* (2012) in Canada (8.31–83.7 ng m^{-3}, sampling time: 2009) or and by Bian *et al.* (2016) in Saudi Arabia (18.4–61.1 ng m^{-3}, sampling time: 2011–2012). The PAH concentrations in industrial site obtained in this study are in the same range of those reported in Kaohsiung, Taiwan (69.3–233 ng m^{-3}) by Lai *et al.* (2017).

The level of atmospheric PAHs depends on various factors including emission sources and meteorological parameters such as rainfall, wind speed, wind direction and temperature, which lead to the seasonal variation of atmospheric PAHs. Numerous studies indicate that PAH concentration in winter (cold season) is higher than that in summer (high-temperature season). Van Drooge *et al.* (2010) indicated that total PAHs concentration in winter is about 5 times higher than that in summer. Liu *et al.* (2008) also reported the levels of PAHs in gas phase and particulate phase are 1.5 and 8 times higher, respectively, if compared with those sampled in summer time. However, this trend is found only for urban site, which is located farther away from the seashore compared with two other sites (Fig. 1). The PAH concentrations are higher in summer than those in winter for rural and industrial sites (Fig. 2), which is consistent with the trend of PCN concentrations measured at the same sites and same sampling period (Dat *et al.*, 2018). In this study, the sampling sites are located in the northern Taiwan, with the air mass mainly originating from the north in the winter and the air mass arising from the south in summer time as presented in Fig. S2, based on 48-hour air mass back-trajectory using the HYSPLIT transport and dispersion model from the NOAA Air Resources Laboratory. As a consequence, the air mass should have traveled a longer distance crossing the densely residential and highly industrialized areas located in the southwest of Taiwan (Figs. 1, S2(b) and S2(c)) in summer time compared with that in winter time (Fig. S2(a)). This is the main reason for the higher concentrations of PAHs in summer compared with those in winter time at the rural and industrial sites and the highest concentration of each site in summer time (Fig. S4) corresponding to the longest journey crossing the polluted zones prior to reaching the sampling the sites (Fig. S2(c)). This phenomenon also explains for the lower annual average PAH concentration measured at industrial site which is located very close to seashore (~1 km) and receives the major air mass from ocean. In case of urban site, Zhongli district is located farther away from the seashore compared with other sites, which means the air mass passing through this sampling site having a longer journey crossing a densely populated area and some

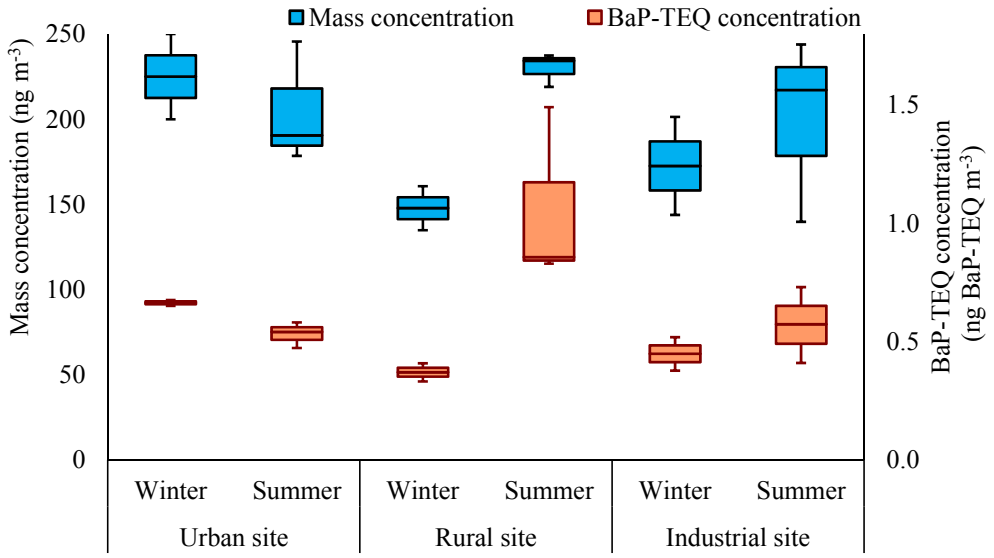

Fig. 2. Mass and BaP-TEQ concentrations of PAHs in winter and summer at three sites.

industrial zone in the north in winter, furthermore, Zhongli district is also of the highest population density in Taoyuan city. These reasons lead to not much difference between air masses received by urban site in the winter and the summer, therefore, the level of atmospheric PAHs at urban site is governed by the trend of the higher PAHs concentration in winter time (low temperature) compared with that in summer time (high temperature). There are several reasons to explain the trend, such as: (1) increase of PAHs emission from enhanced domestic heating demand (Birgul and Tasdemir, 2015) and lower combustion efficiency of vehicular engines (Arhami *et al.*, 2010) during winter time, (2) reduction of atmospheric photo-, thermo- and chemical oxidations due to lower solar radiations in winter time, (3) lower mixing layer and frequent thermal inversion may trap pollutants within low tropospheric layer and reduce their dispersion (Liu *et al.*, 2008; Kong *et al.*, 2010; Masih *et al.*, 2012; Lv *et al.*, 2016; Tomaz *et al.*, 2016).

Positive correlations between total PAHs and SO_x, NO_x are found in the winter (R^2 = 0.48 and 0.53, respectively). However, no significant correlation between total PAHs and criteria pollutants is found in summer. These results suggest that PAHs, SO_x, NO_x are from similar sources in winter. However, the average concentrations of these criteria pollutants in winter are also higher than those measured in summer for all three sites, which reveals opposite trend to total PAHs concentration. This result suggests that evaporation of PAHs in summer time may play an important role.

Gas-phase PAHs predominate in atmosphere, accounting for 98.7–99.0%, 98.4–98.7% and 97.9–98.9% at urban, rural and industrial sites, respectively. The results are consistent with those reported by Lai *et al.* (2017) for 98% and 99.8% of gas-phase PAHs in spring and summer, respectively at industrial sites. Van Drooge *et al.* (2010) also reported that gaseous phase accounts for 72 to 95% of total PAHs observed at remote background sites. Similar results are presented by various studies such as Li *et al.* (2006), Cincinelli *et al.* (2007), Van Drooge *et al.* (2010), Ramirez *et al.* (2011), Hassan and Khoder (2012), Anastasopoulos *et al.* (2012), Masih *et al.* (2012), Birgul and Tasdemir (2015) and Liu *et al.* (2015). Gas-phase PAHs concentrations at three sites in winter and summer follow the trend of total mass concentrations. A different trend is found for particulate-phase PAHs with a comparable level found at the urban site (2.59 ± 0.650 ng m^{-3}) and the industrial site (2.59 ± 0.440 ng m^{-3}), followed by rural site (2.15 ± 0.0201 ng m^{-3}) in winter. However, in summer, the highest particulate-phase PAH concentration is observed at rural site (3.90 ± 0.65 ng m^{-3}), followed by industrial site (2.75 ± 0.650 ng m^{-3}) and urban site (2.26 ± 0.380 ng m^{-3}). The highest annual concentration is observed at rural site (3.20 ± 0.990 ng m^{-3}), followed by industrial site (2.69 ± 0.580 ng m^{-3}) and urban site (2.39 ± 0.530 ng m^{-3}). These particulate PAH concentrations are comparable in the winter and higher than those measured in summer time in Kaohsiung measured in 2012 (1.14 and 0.2 ng m^{-3} for winter and summer, respectively) as reported by Lai *et al.* (2017). Wang *et al.* (2011) indicated that comparable particulate-phase PAH level was also observed in Beijing and significantly higher level of particulate-phase PAHs was found at rural villages, China in winter, with the level of 80–100 times higher than those observed in this study.

In term of BaP-TEQ concentration, the highest BaP-TEQ concentration was found at rural site in summer (1.1 ± 0.3 ng BaP-TEQ m^{-3}), which exceeds 1 ng BaP-TEQ m^{-3} for ambient PAHs standard as recommended by European Commission (European Commission, 2005). This result indicates that the human health effect associated with PAHs exposure in the summer time of population located in northern Taiwan should receive more attention. Furthermore, the average annual concentration of rural site is the highest (0.8 ± 0.4 ng BaP-TEQ m^{-3}), followed by urban site (0.6 ± 0.07 ng BaP-TEQ m^{-3}) and industrial site (0.5 ± 0.1 ng BaP-TEQ m^{-3}). These concentrations are higher than those reported in UK (0.029–2.0 ng BaP-TEQ m^{-3}) by Brown and Brown (2012) and comparable with the concentrations in Kaohsiung, Taiwan (0.084–1.51 ng BaP-TEQ m^{-3}), as observed by Lai *et al.* (2017). However, these concentrations are significantly lower than those reported at a rural village (up to 35 ng BaP-TEQ m^{-3}) in China by Wang *et al.* (2011). The concentrations of BaP and DahA (with the highest TEF) in summer time are higher than those in winter time, resulting in higher total BaP-TEQ concentration in summer than in winter for rural and industrial sites.

PAH Congeners Distributions

Generally, low-ring PAHs (2, 3-ring PAHs) predominate in gas phase and high-ring PAHs (5, 6-ring PAHs) dominate in particulate phase while medium-ring PAHs (4-ring PAHs) are associated with both gas and particle phases. As presented in Fig. 3, NAP (2-ring PAH) predominates in gas phase, accounting for 83 ± 8% in winter and 89 ± 4% in summer, followed by 3-ring PAHs, composing for 12 ± 6% in winter and 7 ± 2% in summer and 4-ring PAHs, making up 5 ± 2% in winter and 4 ± 2% in summer. PHE is of the highest contribution among 3-ring PAHs (6 ± 4%), followed by FLT (2 ± 1%), PYR (2 ± 1%) and FLU (2 ± 1%). For particulate-phase PAHs, 4-ring- and 5-ring- PAHs dominate in winter, accounting for 30 ± 7% and 28 ± 8%, respectively, followed by 6-ring PAHs (23 ± 6%). However, in the summer, 6-ring PAHs are the main contributors (51 ± 9%), followed by 5-ring PAHs (30 ± 6%) and 4-ring PAHs (13 ± 5%). IcdP is the most contributor to particle-phase PAHs (22 ± 9%), followed by BghiP (17 ± 7%) and BbF (15 ± 3%) (Fig. 3(b)), which are consistent with those reported by Liu *et al.* (2016). These results are in agreement with those observed by Zhu *et al.* (2014) with the significantly lower contributions of low-ring PAHs to particulate-phase PAHs in the summer (2 ± 1% and 4 ± 2% for NAP and 3-ring PAHs, respectively) compared with those in winter (9 ± 9% and 10 ± 9% for NAP and 3-ring PAHs, respectively). This trend indicates the increasing volatilization of low-ring PAHs which are more volatile from particle to gas phase in the summer which was also reported by Kong *et al.* (2010).

Gas-phase PAH distributions in winter at urban and rural sites are comparable, which are different from those observed at industrial site with the lower distribution of

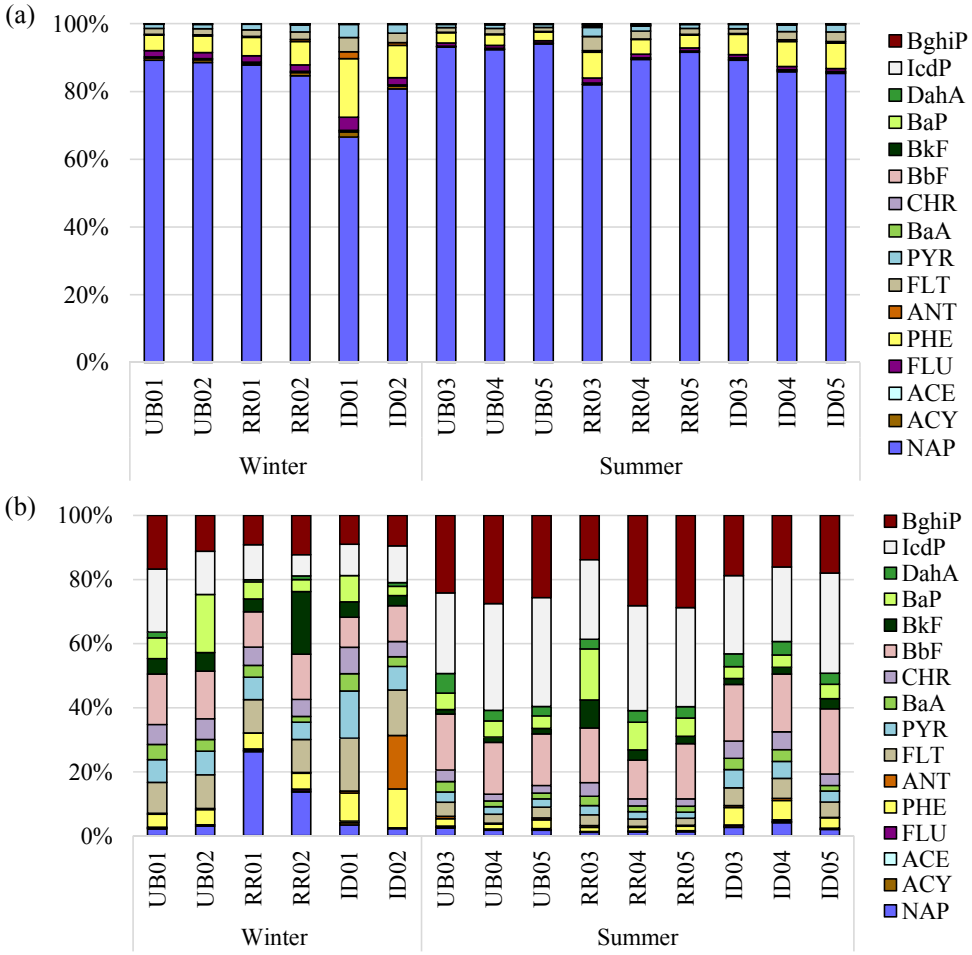

Fig. 3. PAHs distribution in gas a) and particulate b) phases. (UB: Urban site, RR: rural site, ID: industrial site; 01, 02 are the samples collected in winter and 03, 04, 05 are the samples collected in summer).

NAP and higher contributions of 3- and 4-ring PAHs. The highest concentration of total 7 PAHs congeners (ACY, ACE, FLU, PHE, ANT, FLT, PYR) were also observed for the sample ID01, indicating that different sources contribute to PAHs measured at these sites. The gas-phase PAH distributions in summer are quite similar for rural and industrial sites, however, a higher contribution of NAP is observed in urban site compared with two other sites (Fig. 3(a)). The particle-phase PAH distributions are quite similar among three sampling sites within each season. Particles collected at rural site have higher contribution of NAP (20% on average) compared with those of other sites (lower than 3%). The contribution of 3- and 4-ring PAHs at industrial site are higher than those at other sites (Fig. 3(b)). Significantly higher concentration of DahA was found in summer (0.0801–0.140 ng m^{-3}) compared with that measured in winter (n.d–0.0601 ng m^{-3}). These results suggest that various sources contribute to the PAHs collected at different sites in different seasons.

Particulate-phase PAHs dominate BaP TEQ distribution, accounting for 51.3–75.1%, except for the sample ID01 (46.3%). Significantly higher contribution of particulate-phase to total TEQ concentration is also reported by various studies such as Akyüz and Çabuk (2010) (up to 86%), Wang *et al.* (2011) (98%), Chen *et al.* (2011) (up to 94%) because of the higher association with particles of HMW-PAHs which are of high TEF values. However, due to the predominance of NAP in gas phase, NAP is also the main contributor to the gas-phase TEQ concentration, accounting for 47.5–85.0%. HMW-PAHs with higher TEF values are major contributors of particulate PAHs, including BaP accounting for 47 ± 16%, followed by DahA (19 ± 11%), BghiP (14 ± 4.8%) and BbF (12 ± 3.1%).

Diagnostic Ratios and Potential Sources of PAHs

Diagnostic ratios are applied effectively as indicators of PAH sources by various studies (Ravindra *et al.*, 2008; Dvorská *et al.*, 2011; Katsoyiannis *et al.*, 2011; Tobiszewski and Namiesnik, 2012; Kuo *et al.*, 2013; Kamal *et al.*, 2016; Chen *et al.*, 2017; Saha *et al.*, 2017) based on the relative thermodynamic stability of different parent PAHs and the characteristics of different PAHs sources (Bian *et al.*, 2016). In this study, the diagnostic ratios of FLA/(FLA + PYR), ANT/(ANT + PHE), BaA/(BaA + CHR) and IcdP/(IcdP + BghiP) are employed to identify possible PAH sources of the samples collected as shown in Fig. 4. ANT/(ANT + PHE) ratio was usually used to distinguish the source between petroleum combustion and evaporation (Callen *et*

2011). The ratio of ANT/(ANT + PHE) < 0.1 indicates petroleum evaporation while ratio > 0.1 is for petroleum combustion. FLA/(FLA + PYR) > 0.5 indicates grass, wood, coal combustion, while FLA/(FLA + PYR) < 0.4 is mainly for petrogenic source and 0.4 > FLA/(FLA + PYR) > 0.5 for fossil fuel combustion (De La Torre-Roche *et al.*, 2009). As shown in Fig. 4(a), only two samples (ID01 and ID02) are located in different region from other samples, which indicates that ID01 and ID02 were influenced by combustions of solid fuel and petroleum. While other samples with low ratio of ANT/(ANT + PHE) (< 0.1) and high ratio of FLA/(FLA + PYR) (> 0.5) indicate the influence of petroleum evaporation (Bian *et al.*, 2016). The scatter plot of BaA/(BaA + CHR) and IcdP/(IcdP + BghiP) ratios is presented in Fig. 4(b). BaA/(BaA + CHR) < 0.2 indicates petroleum evaporation, BaA/(BaA + CHR) = 0.2–0.35 is from coal combustion and BaA/(BaA + CHR) > 0.35 is related to vehicular emission or combustion (Akyüz and Çabuk, 2010, Yunker *et al.*, 2002). IcdP/(IcdP + BghiP) < 0.2 indicates petrogenic source, IcdP/(IcdP + BghiP) = 0.2–0.5 is petroleum combustion and IcdP/(IcdP + BghiP) > 0.5 is grass, wood and coal combustion (Yunker *et al.*, 2002). As shown in Fig. 4(b), all samples measured in winter are related to the combustion of solid fuels including grass, wood, coal/petroleum and vehicular emission. While most of the samples collected in summer are influenced by evaporation and combustion of petroleum, only UB04 is related to petroleum evaporation and coal combustion. Obviously, different source compositions contribute to PAHs measured in winter and summer. All samples collected at industrial site in two seasons are related to combustion of solid fuel and petroleum. Samples collected in winter at rural and urban sites are influenced by mixed sources of solid fuel/petroleum combustions and petroleum evaporation. Rural and urban sites are more related to petroleum evaporation, however, solid fuel/petroleum combustion or vehicular emission also influences these sites in summer.

Gas/Particle Partitioning of Atmospheric PAHs

Gas/Particle Partitioning and $logK_p$-$logP^0_L$ Relationship

Gas-particle partitioning of PAHs can be evaluated by $logK_p$ value. K_p is the gas-particle partitioning coefficient ($m^3\ \mu g^{-1}$) which can be calculated via Eq. (1) (Introduction section) following Pankow (1987). Results show that $logK_p$ increases from –5.35 to 0.230 as the ring number of PAHs increases from 2 to 5, which indicates that heavier PAHs have *al.*, 2011). The ratio of ANT/(ANT + PHE) < 0.1 indicates petroleum evaporation while ratio > 0.1 is for petroleum

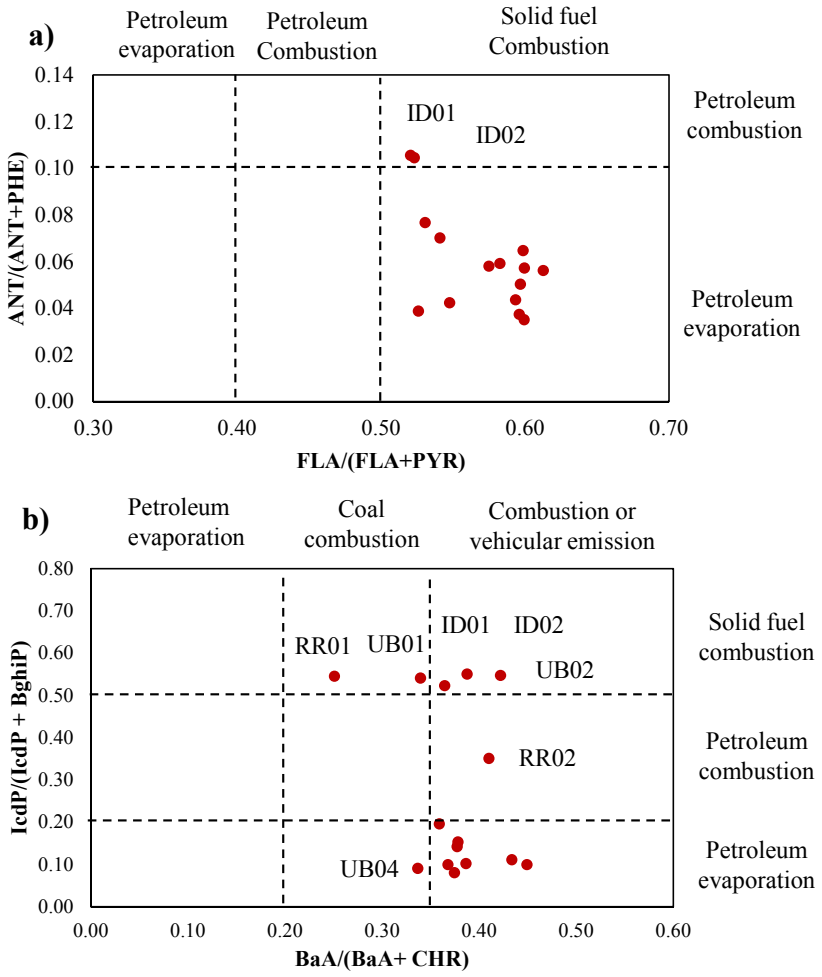

Fig. 4. Diagnostic ratios of FLA/(FLA + PYR) and ANT/(ANT + PHE) (a) BaA/(BaA + CHR) and IcdP/(IcdP + BghiP) (b)

higher tendency to associate with particles. $\log K_p$ values range from –5.1 to –0.7 and –5.4 to –1.1 in winter and summer, respectively, for 2-ring to 6-ring PAHs. $\log K_p$ values are higher in winter compared with those in summer which is consistent with the temperature-dependence of gas/particle partitioning as performed firstly by Yamasaki *et al.* (1982) with the relation $\log K_p = m(1/T) + b$, K_p (m^3 μg^{-1}) is the gas/particle partitioning coefficient defined by Eq. (1), m and b are empirical constants related to the heat of PAH phase change and the properties of individual PAH and the particulate matter. Therefore, a compound with a higher K_p value has a higher tendency to associate with particulate matter and the equilibrium shifts towards PAHs in the particulate phase when ambient temperature decreases. Various studies report that higher $\log K_p$ values are measured in the winter than those in the summer and high-molecular-weight PAHs have high $\log K_p$ values, which are consistent with those obtained in this study (Terzi and Samara, 2004; Akyüz and Çabuk, 2010; Yang *et al.*, 2010b; Wang *et al.*, 2011, Yu and Yu, 2012; Carreras *et al.*, 2013; Zhu *et al.*, 2014).

The relationships between $\log K_p$ and $\log P^0_L$ (calculated following Odabasi *et al.*, 2006) of different sites in winter and summer are presented in Fig. 5, and the correlations between $\log K_p$ and $\log P^0_L$ (R^2 = 0.835–0.950) are significant in all three sites. Generally, the slope values for three sites in winter are comparable (–0.774 to –0.716) which are closer to –1 if compared with those observed in summer (–0.629 to –0.532), indicating that the gas/particle partitioning of PAHs in winter are closer to equilibrium state than in summer. The slope values ranging from –0.774 to –0.716 also indicate that both adsorption and absorption govern the gas/particle partitioning of PAHs in winter. The slope values of urban and rural sites in summer (–0.532 and –0.551, respectively) indicate that absorption is the major mechanism governing the gas/particle partitioning of PAHs at urban and rural sites in summer. Slope value of –0.629 reveals that both adsorption and absorption are involved with the gas/particle partitioning of PAHs at industrial site in summer. This trend was also found by Wei *et al.* (2015) with the slopes closer to –1 in March (lower temperature) compared with those in September (higher temperature) and stronger absorption was found in September to govern gas/particle partitioning. Wang *et al.* (2011) and Wang *et al.* (2013) also indicated that both adsorption and absorption simultaneously govern the gas/particle partitioning of PAHs. The sorption and desorption of newly released PAHs onto and from aerosols may take hours to reach equilibrium during transportation (Dachs and Eisenreich, 2000), therefore, the results also indicate that PAHs collected in summer time could be more related to the local emissions compared with those in winter. Another possibility is the lower $\log K_p$ values in summer time compared with those in winter time, resulting in less negative of slope values in summer time (Wei *et al.*, 2015).

Comparison of Different Gas/Particle Partitioning Models

A most common approach for calculating the

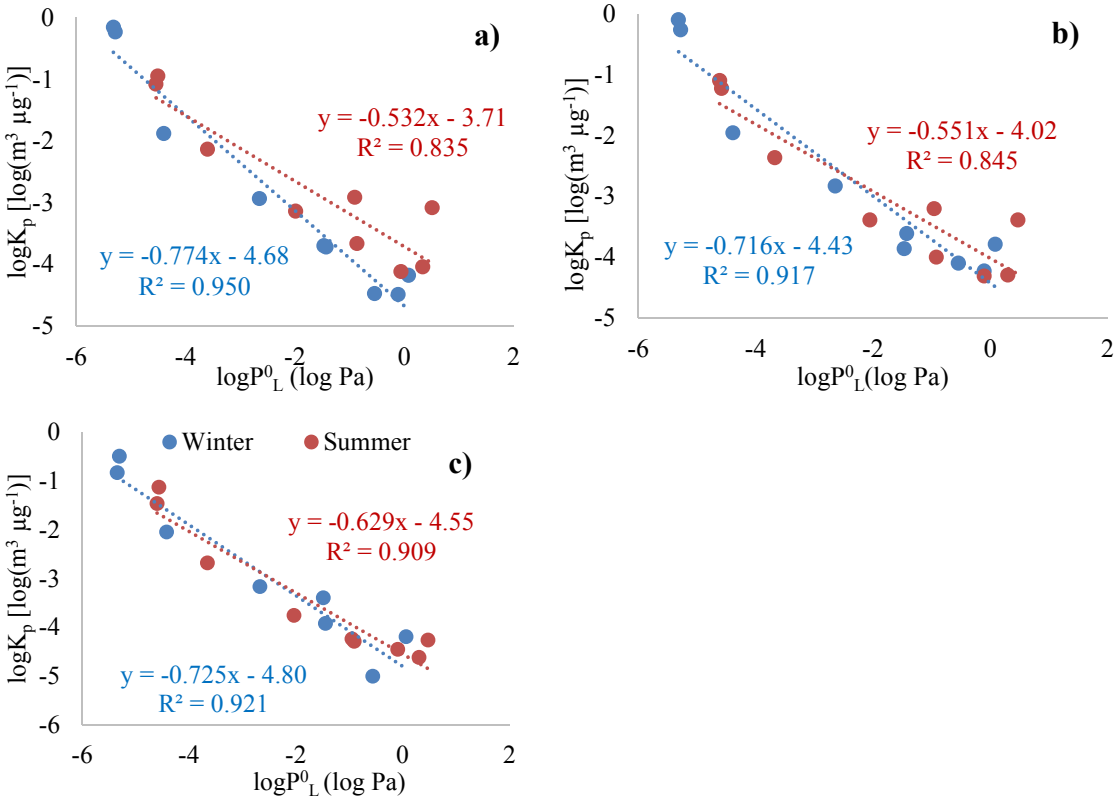

Fig. 5. $\log K_p$-$\log P^0_L$ relationship based on calculated $\log K_p$, $\log P^0_L$ of PHE, ANT, FLT, CHR, BbF, BkF (a, b, c refer to urban, rural and industrial sites, respectively).

gas/particle partitioning of SVOCs is Junge-Pankow (J-P) model which assumes adsorption of SVOCs onto aerosol is the main mechanism (Pankow, 1987). In this model, fraction of SVOCs in particulate phase is estimated by Eq. (3):

$$\varphi = c\theta/(p^0_L + c\theta) \quad (3)$$

where θ is particle surface area per unit of air volume ($cm^2\ cm^{-3}$), and is assumed as 1.1×10^{-5} ($cm^2\ cm^{-3}$) for urban air, 2.5×10^{-6} ($cm^2\ cm^{-3}$) in range of 1.0–3.5×10^{-6} ($cm^2\ cm^{-3}$) for rural air and 1.0×10^{-7} ($cm^2\ cm^{-3}$) for remote air (Lohmann and Lammel, 2004), and c is a constant related to the properties of the compounds of interest and is often assumed to be 17.2 Pa cm for PAHs (Wang *et al.*, 2013).

Absorption K_{OA} model is proposed by Harner and Bidleman (1998) with the assumption that absorption of SVOCs onto OM phase of aerosol is the main mechanism governing gas/particle partitioning. In this model, the relationship between K_p and K_{OA} is expressed as Eq. (4):

$$K_p = f_{OM}\frac{\zeta_{OCT}}{\zeta_{OM}}\frac{MW_{OCT}}{\rho_{OCT}MW_{OM}10^{12}}K_{OA} \quad (4)$$

where f_{OM} is the fraction of OM in aerosol, MW_{OTC} and MW_{OM} are the mean molecular weights of octanol and OM, ζ_{OCT} and ζ_{OM} are activity coefficients of the absorbing compound in octanol and OM, ρ_{OTC} is the density of octanol (0.82 kg L^{-1} at 20°C) and the factor 10^{12} converts units of the right-hand side of the equation from L kg^{-1} to $m^3\ \mu g^{-1}$. K_{OA} is the octanol-air partitioning coefficient calculated following Odabasi (2006). With the assumptions of $MW_{OCT}/MW_{OM} = 1$ and $\zeta_{OCT}/\zeta_{OM} = 1$, Eq. (4) can be simplified as:

$$\log K_p = \log K_{OA} + \log f_{OM} - 11.91 \quad (5)$$

Air-soot model proposed by Dachs and Eisenreich (2000) combines the effects of soot on the gas/particle partitioning of PAHs. The overall gas/particle partitioning coefficient that includes both OM and the soot phases is expressed as the Eq. (6):

$$K_p = f_{OM}\frac{\zeta_{OCT}}{\zeta_{OM}}\frac{MW_{OCT}}{\rho_{OCT}MW_{OM}10^{12}}K_{OA} + f_{EC}\frac{\alpha_{EC}}{\alpha_{AC}10^{12}}K_{SA} \quad (6)$$

where K_{SA} is the soot-air partition coefficient, f_{EC} is the fraction of elemental carbon in the aerosol, and α_{EC} and α_{AC} are specific surface areas of elemental carbon and activated carbon, respectively.

The value of K_{SA} for different PAHs can be estimated by the Eq. (7) as established by Van Noort (2003):

$$\log K_{SA} = -0.85\log P_L^0 + 8.94\log 998/\alpha_{EC} \quad (7)$$

As mentioned previously, the following assumption can be adopted: $\zeta_{OCT}/\zeta_{OM} = 1$, $\alpha_{EC}/\alpha_{AC} = 1$, $MW_{OCT}/MW_{OM} = 1$. In this study, the value of α_{EC} was taken as 100 $m^2\ g^{-1}$ from Bucheli and Gustafsson (2000).

The estimated fraction of PAHs in particulate phase can be calculated by the Eq. (8) based on K_p value obtained from previous steps and TSP concentration:

$$\varphi = C_p/(C_p + C_g) = K_p(TSP)/[1 + K_p(TSP)] \quad (8)$$

Results from J-P adsorption model are based on θ value corresponding to urban air (1.1×10^{-5} $cm^2\ cm^{-3}$) because the φ values calculated using this θ value are closer to the φ observed. The values of f_{OM} and f_{EC} used for calculating K_p in soot-air model are 0.1 and 0.035, respectively, based on the characteristics of particulate matter collected in northern Taiwan. As presented in Table 1, the estimated φ using J-P adsorption model are closer to φ observed compared with those calculated by K_{OA} absorption model in both winter and summer, which indicates that the adsorption onto particle surface is more important than the absorption of OM phase. The estimated φ values calculated using soot-air model are significantly closer to the measured φ values ($\varphi_{observed}/\varphi_{estimated}$ ratios closer to 1) compared with those calculated following absorption K_{OA} model and J-P adsorption model (especially for ACY and ACE), which is consistent with that reported by Wang *et al.* (2013). This result is in agreement with the conclusion that the adsorption of soot carbon plays an important role on gas/particle partitioning of PAHs and absorption is the main mechanism governing gas/particle partitioning only when OC content of aerosol is 100 times higher than EC content (Dachs and Eisenreich, 2000; Callén *et al.*, 2008). On the other hand, in this study, the estimated φ values were calculated by some fixed parameters as presented previously. However, different sources might contribute to particulate matters in different seasons, which means different aerosol characteristics between winter and summer. The fractions of EC and OC differ in two seasons and even for similar fractions of EC and OC, different soot-carbon origins also lead to different results of estimated φ (Callen *et al.*, 2008). This may be the reason for higher ratios ($\varphi_{observed}/\varphi_{estimated}$) in summer compared with those in winter for all models.

Furthermore, Table 1 also shows that the $\varphi_{observed}/\varphi_{estimated}$ ratios of 5- and 6- ring PAHs (BbF to BghiP) are comparable and approach to 1 for all three models. This result reveals that the gas/particle partitioning of HMW-PAHs which are of high K_p values seem independent from whether adsorption or adsorption governing the gas/particle partitioning. In fact, HMW-PAHs associate with particulate phase very fast by self-condensation on existing aerosol surface due to very low vapor pressures ($< 10^{-4.5}$ Pa in this study). It is also noted that 4 congeners (BaP to BghiP) are not found in gas phase, and BbF and BkF are found in particulate phase with very low concentrations.

Table 2 compares the $\varphi_{observed}/\varphi_{estimated}$ ratios of different sites in winter and summer obtained by the soot-air model. In fact, all models used in this study are based on the assumption that equilibrium state is reached between gas and particulate phases. Obviously, the ratios corresponding to samples collected in winter are closer to 1 than those in summer time, which indicates that the gas/particle partitioning of PAHs is closer to equilibrium in winter than those on

Table 1. Results of $\varphi_{observed}/\varphi_{estimated}$ ($\varphi_{obs.}/\varphi_{est.}$) obtained from three models: J-P adsorption model, K_{OA} absorption model and soot-air model ($f_{OM} = 0.1$, $f_{EC} = 0.035$).

PAHs	J-P model		Absorption K_{OA} model		Soot-air model	
	Winter	Summer	Winter	Summer	Winter	Summer
	$\varphi_{obs.}/\varphi_{est.}$	$\varphi_{obs.}/\varphi_{est.}$	$\varphi_{obs.}/\varphi_{est.}$	$\varphi_{obs.}/\varphi_{est.}$	$\varphi_{obs.}/\varphi_{est.}$	$\varphi_{obs.}/\varphi_{est.}$
ACY	50	328	243	2215	4.3	38
ACE	16	35	77	186	1.4	3.4
FLU	4.0	16	27	77	0.50	1.5
PHE	2.5	5.1	16	31	0.40	0.70
ANT	8.9	19	47	153	1.2	3.6
FLT	0.90	1.4	6.5	9.7	0.30	0.30
CHR	0.50	0.50	1.4	2.9	0.50	0.30
BbF	1.0	0.90	1.1	1.8	1.0	0.90
BkF	1.0	0.90	1.1	1.7	1.0	0.90
BaP	1.0	1.1	1.1	1.8	1.0	1.1
DahA	0.70	1.0	0.70	1.1	0.70	1.0
IcdP	1.0	1.0	1.0	1.1	1.0	1.0
BghiP	1.0	1.0	1.0	1.1	1.0	1.0

Table 2. Comparison of $\varphi_{observed}/\varphi_{estimated}$ ratios calculated for different sites in winter and summer using the soot-air model.

PAHs	Urban site		Rural site		Industrial site	
	Winter	Summer	Winter	Summer	Winter	Summer
ACY	3.0	77	6.7	34	2.5	4.3
ACE	1.0	5.9	1.8	3.0	n.a	1.3
FLU	0.38	2.3	0.91	1.4	0.12	0.87
PHE	0.39	1.4	0.50	0.56	0.33	0.27
ANT	0.38	7.2	0.26	3.0	3.0	0.40
FLT	0.26	0.51	0.32	0.25	0.19	0.14
CHR	0.47	0.38	0.40	0.25	0.50	0.34
BbF	0.98	0.90	1.0	0.74	0.96	0.96
BkF	0.97	0.84	1.0	0.82	0.93	0.90
BaP	1.0	1.1	1.0	1.1	0.94	1.0
DahA	1.0	1.0	1.0	1.0	1.0	1.0
IcdP	1.0	1.0	1.0	1.0	0.96	1.0
BghiP	1.0	1.0	1.0	1.0	1.0	1.0

n.a: not available.

summer. This trend is consistent with the slope values of $\log K_p$–$\log P^0_L$ relationships, which are closer to –1 in winter than those in summer. Furthermore, the over- and under-estimated φ may indicate that the corresponding PAHs do not reach equilibrium between gas and particulate phases. Dachs and Eisenreich, (2000) indicate that the sorption and desorption of newly released PAHs onto and from aerosols may take hours to reach equilibrium. The ratios corresponding to ACY and ACE are significantly higher than 1, possibly due to dominance of these congeners in particulate phase released from PAH sources nearby. The fractions corresponding to FLU, PHE, ANT, FLT, CHR are mostly lower than 1 in winter at three sites and in summer at industrial site, which suggesting that these congeners maybe dominant in gas-phase PAHs in emission sources.

CONCLUSION

Overall, urban site is of the highest PAHs mass concentration, followed by rural and industrial sites. In winter, the highest concentration was observed at urban site (200–250 ng m^{-3}), followed by industrial site (201–144 ng m^{-3}) and rural site (135–161 ng m^{-3}). However, in summer, rural site has the highest PAHs concentration (219–237 ng m^{-3}), followed by urban site (179–246 ng m^{-3}) and industrial site (140–244 ng m^{-3}). The PAHs concentration at urban site in winter is higher than that in summer. At rural and industrial sites, PAHs concentrations measured in summer are higher than those in winter due to the longer journey of air mass crossing residential and industrial areas prior to reaching the sampling sites in summer. The average BaP-TEQ concentration at rural site is the highest in summer, followed by urban and industrial sites, due to high concentrations of BaP and DahA, which are of the highest TEF values. This result suggests that the human exposure to PAHs in summer time should receive more attention. Sources of PAHs collected might be different at different sites in winter and summer time. All samples collected at industrial site in two seasons are related to the combustion of solid fuel and petroleum. On the other hand, all samples

collected in winter at rural and urban sites are influenced by mixed sources of solid fuel/petroleum combustions and petroleum evaporation. Rural and urban sites are more related to petroleum evaporation, however, solid fuel/petroleum combustions or vehicular emissions also influence on these sites in summer. Gas/particle partitionings are similar at three sites in winter, while those at industrial site in summer differs from urban and rural sites. The comparison between different models for evaluating gas/particle partitioning indicates that both adsorption and absorption might govern gas/particle partitioning of PAHs at three sites, however, adsorption onto soot carbon is a more important mechanism in governing gas/particle partitioning of PAHs collected.

ACKNOWLEDGEMENTS

The authors gratefully acknowledge the financial supports provided by the Taiwan EPA and the Ministry of Science and Technology (MOST-105-EPA-F-005-003, MOST-105-2622-8-009-007-TE4 and MOST 105-221-E-008-006-MY3). The supports provided by Prof. Kai-Hsien Chi and Mr. Chian-Kou Lien of National Yang-Ming University for sampling are valuable and acknowledged.

SUPPLEMENTARY MATERIAL

Supplementary data associated with this article can be found in the online version at http://www.aaqr.org.

REFERENCES

Akyüz, M. and Çabuk, H. (2010). Gas-particle partitioning and seasonal variation of polycyclic aromatic hydrocarbons in the atmosphere of Zonguldak, Turkey. *Sci. Total Environ.* 408: 5550–5558.

Allen, J.O., Dookeran, N.M., Smith, K.E., Sarofilm, A.F., Taghizadeh, K. and Lafeur A.L. (1996). Measurement of polycyclic aromatic hydrocarbons associated with size segregated atmospheric aerosols in Massachusetts. *Environ. Sci. Technol.* 30: 1023–1031.

Anastasopoulos, A.T., Wheeler, A.J., Karman, D. and Kulka, R.H. (2012). Intraurban concentrations, spatial variability and correlation of ambient polycyclic aromatic hydrocarbons (PAH) and $PM_{2.5}$. *Atmos. Environ.* 59: 272–283.

Arhami, M., Minguillon, M.C., Polidori, A., Schauer, J.J., Delfino, R.J. and Sioutas, C. (2010). Organic compound characterization and source apportionment of indoor and outdoor quasi-ultrafine particulate matter in retirement homes of the Los Angeles Basin. *Indoor Air* 20: 17–30.

Bian, Q., Alharbi, B., Jeffrey Collett, J., Kreidenweis, S. and Pasha, M.J. (2016). Measurements and source apportionment of particle-associated polycyclic aromatic hydrocarbons in ambient air in Riyadh, Saudi Arabia. *Atmos. Environ.* 137: 186–198.

Birgul, A. and Tasdemir, Y. (2015). Concentrations, gas-particle partitioning, and seasonal variations of polycyclic aromatic hydrocarbons at four sites in Turkey. *Arch. Environ. Contam. Toxicol.* 68: 46–63.

Brown, A.S. and Brown, R.J. (2012). Correlations in polycyclic aromatic hydrocarbon (PAH) concentrations in UK ambient air and implications for source apportionment. *J. Environ. Monit.* 14: 2072–2082.

Bucheli, T.D. and Gustafsson, O. (2000). Quantification of the soot-water distribution coefficient of PAHs provides mechanistic basis for enhanced sorption observations. *Environ. Sci. Technol.*34: 5144–5151.

Callén, M.S., de la Cruz, M.T., López, J.M., Murillo, R., Navarro, M.V. and Mastral, A.M. (2008). Some inferences on the mechanism of atmospheric gas/particle partitioning of polycyclic aromatic hydrocarbons (PAH) at Zaragoza (Spain). *Chemosphere* 73: 1357–1365.

Callen, M.S., Lopez, J.M. and Mastral, A.M. (2011). Characterization of PM_{10}-bound polycyclic aromatic hydrocarbons in the ambient air of Spanish urban and rural areas. *J. Environ. Monit.* 13: 319–327.

Carreras, H.A., Calderón-Segura, M.E., Gómez-Arroyo, S., Murillo-Tovar, A. and Amador-Muñoz, O. (2013). Composition and mutagenicity of PAHs associated with urban airborne particles in Córdoba, Argentina. *Environ. Pollut.* 178: 403–410.

Chen, P., Li, C., Kang, S., Rupakheti, M., Panday, A.K., Yan, F., Li Q., Zhang, Q., Guo, J., Ji, Z., Rupakheti, D. and Luo, W. (2017). Characteristics of particulate-phase polycyclic aromatic hydrocarbons (PAHs) in the atmosphere over the Central Himalayas. *Aerosol Air Qual. Res.* 17: 2942–2954.

Chen, Y., Feng, Y., Xiong, S., Liu, D., Wang, G., Sheng, G. and Fu, J. (2011). Polycyclic aromatic hydrocarbons in the atmosphere of Shanghai, China. *Environ. Monit. Assess.* 172: 235–247.

Chen, Y.C., Chiang, H.C., Hsu, C.Y., Yang, T.T., Lin, T.Y., Chen, M.J., Chen, N.T. and Wu, Y.S. (2016). Ambient $PM_{2.5}$-bound polycyclic aromatic hydrocarbons (PAHs) in Changhua County, central Taiwan: Seasonal variation, source apportionment and cancer risk assessment. *Environ. Pollut.* 218: 372–382.

Cheruyiot, N.K., Lee, W.J., Mwangi, J.K., Wang, L.C., Lin, N.H, Lin, Y.C, Cao, J., Zhang, R. and Chang-Chien, G.P. (2015). An Overview: polycyclic aromatic hydrocarbon emissions from the stationary and mobile sources and in the ambient air. *Aerosol Air Qual. Res.* 15: 2730–2762.

Cincinelli, A., Bubba, M.D., Martellini, T., Gambaro, A. and Lepri, L. (2007). Gas-particle concentration and distribution of n-alkanes and polycyclic aromatic hydrocarbons in the atmosphere of Prato (Italy). *Chemosphere* 68: 472–478.

Cristale, J., Silva, F.S., Zocolo, G.J. and Marchi, M.R.R. (2012). Influence of sugarcane burning on indoor/outdoor PAH air pollution in Brazil. *Environ. Pollut.* 169: 210–216.

Dachs, J. and Eisenreich, S.J. (2000). Adsorption onto aerosol soot carbon dominates gas-particle partitioning of polycyclic aromatic hydrocarbons. *Environ. Sci. Technol.* 34: 3690–3697.

Dat, N.D. and Chang, M.B. (2017). Review on characteristics of PAHs in atmosphere, anthropogenic

sources and control technologies. *Sci. Total Environ.* 609: 682–693.

Dat, N.D., Chang, K.S. and Chang, M.B. (2018). Characteristics of atmospheric polychlorinated naphthalenes (PCNs) collected at different sites in northern Taiwan. *Environ. Pollut.* 237: 186–195.

Dvorská, A., Komprdová, K., Lammel, G., Klánová, J. and Plachá, H. (2012). Polycyclic aromatic hydrocarbons in background air in central Europe - Seasonal levels and limitations for source apportionment. *Atmos. Environ.* 46: 147–154.

Dvorská, A., Lammel, G. and Klánová, J. (2011). Use of diagnostic ratios for studying source apportionment and reactivity of ambient polycyclic aromatic hydrocarbons over Central Europe. *Atmos. Environ.* 45: 420–427.

Elorduy, I., Elcoroaristizabal, S., Durana, N., García, J.A. and Alonso, L. (2016). Diurnal variation of particle-bound PAHs in an urban area of Spain using TD-GC/MS: Influence of meteorological parameters and emission sources. *Atmos. Environ.* 138: 87–98.

European Commission (2005). Directive 2004/107/EC of the European Parliament and of the Council of 15 December 2004 relating to arsenic, cadmium, mercury, nickel and polycyclic aromatic hydrocarbons in ambient air. Official Journal of the European Union, L 023, 0003-0016.

Finzio, A., Mackay, D., Bidleman, T.F. and Harner, T. (1997). Octanol–air partition coefficient as a predictor of partitioning of semivolatile organic chemicals to aerosols. *Atmos. Environ.* 31: 2289–2296.

Garrido, A., Jimenez-Guerrero, P. and Ratola, N. (2014). Levels, trends and health concerns of atmospheric PAHs in Europe. *Atmos. Environ.* 99: 474–484.

Goss, K.U. and Schwarzenbach, R.P. (1998). Gas/solid and gas/liquid partitioning of organic compounds: Critical evaluation of the interpretation of equilibrium constants. *Environ. Sci. Technol.* 32: 2025–2032.

Gregoris, E., Argiriadis, E., Vecchiato, M., Zambon, S., Pieri, S.D., Donateo, A., Contini, D., Piazza, R., Barbante, C. and Gambaro, A. (2014). Gas-particle distributions, sources and health effects of polycyclic aromatic hydrocarbons (PAHs), polychlorinated biphenyls (PCBs) and polychlorinated naphthalenes (PCNs) in Venice aerosols. *Sci. Total Environ.* 476–477: 393–405.

Hafner, W.D., Carlson, D.L. and Hites, R.A. (2005). Influence of local human population on atmospheric polycyclic aromatic hydrocarbon concentrations. *Environ. Sci. Technol.* 39: 7374–7379.

Harner, T. and Bidleman, T.F. (1998). Octanol–air partition coefficient for describing particle/gas partitioning of aromatic compounds in urban air. *Environ. Sci. Technol.* 32: 1494–1502.

Hassan, S.K. and Khoder, M.I. (2012). Gas–particle concentration, distribution, and health risk assessment of polycyclic aromatic hydrocarbons at a traffic area of Giza, Egypt. *Environ. Monit. Assess.* 184: 3593–3612.

Kamal, A., Syed, J.H., Li, J., Zhang, G., Mahmood, A. and Malik R.N. (2016). Profile of atmospheric PAHs in Rawalpindi, Lahore and Gujranwala Districts of Punjab Province (Pakistan). *Aerosol Air Qual. Res.* 16: 1010–1021.

Katsoyiannis, A., Sweetman, A.J. and Jones, K.C. (2011). PAH molecular diagnostic ratios applied to atmospheric sources: A critical evaluation using two decades of source inventory and air concentration data from the UK. *Environ. Sci. Technol.* 45: 8897–8906.

Kong, S., Ding, X., Bai, Z., Han, B., Chen, L., Shi, J. and Li, Z. (2010). A seasonal study of polycyclic aromatic hydrocarbons in $PM_{2.5}$ and $PM_{2.5–10}$ in five typical cities of Liaoning Province, China. *J. Hazard. Mater.* 183: 70–80.

Kuo, C.Y., Chien, P.S., Kuo, W.C., Wei, C.T. and Rau, J.Y. (2013). Comparison of polycyclic aromatic hydrocarbon emissions on gasoline- and diesel-dominated routes. *Environ. Monit. Assess.* 185: 5749–5761.

Lai, Y.C, Tsai, C.H., Chen, Y.L. and Chang-Chien, G.P. (2017). Distribution and sources of atmospheric polycyclic aromatic hydrocarbons at an industrial region in Kaohsiung, Taiwan. *Aerosol Air Qual. Res.* 17: 776–787.

Liu, L.Y., Kukucka, P., Venier, M., Salamova, A., Klanova, J. and Hites, R.A. (2014). Differences in spatiotemporal variations of atmospheric PAH levels between North America and Europe: Data from two air monitoring projects. *Environ. Int.* 64: 48–55.

Liu, S., Tao, S., Liu, W., Dou, H., Liu, Y., Zhao, J., Little, M.G., Tian, Z., Wang, J., Wang, L. and Gao, Y. (2008). Seasonal and spatial occurrence and distribution of atmospheric polycyclic aromatic hydrocarbons (PAHs) in rural and urban areas of the North Chinese Plain. *Environ. Pollut.* 156: 651–656.

Liu, X., Li, C., Tu, H., Wu, Y., Ying, C., Huang, Q., Wu, S., Xie, Q., Yuan, Z. and Lu, Y. (2016). Analysis of the effect of meteorological factors on $PM_{2.5}$-associated PAHs during autumn-winter in urban Nanchang. *Aerosol Air Qual. Res.* 16: 3222–3229.

Liu, Y., Wang, S., Lohmann, R., Yu, N., Zhang, C., Gao, Y., Zhao, J. and Ma, L. (2015). Source apportionment of gaseous and particulate PAHs from traffic emission using tunnel measurements in Shanghai, China. *Atmos. Environ.* 107: 129–136.

Lv, Y., Li, X., Xu, T.T., Cheng, T.T., Yang, X., Chen, J.M., Iinuma, Y. and Herrmann, H. (2016). Size distributions of polycyclic aromatic hydrocarbons in urban atmosphere: Sorption mechanism and source contributions to respiratory deposition. *Atmos. Chem. Phys.* 16: 2971–2983.

Masih, J., Singhvi, R., Taneja, A., Kumar, K. and Masih, H. (2012). Gaseous/particulate bound polycyclic aromatic hydrocarbons (PAHs), seasonal variation in North central part of rural India. *Sustain. Cities Soc.* 3: 30–36.

Odabasi, M., Cetin, E. and Sofuoglu, A. (2006). Determination of octanol-air partition coefficients and supercooled liquid vapor pressures of PAHs as a function of temperature: application to gas-particle partitioning in an urban atmosphere. *Atmos. Environ.* 40: 6615–6625.

Pankow, J.F. (1987). Review and comparative analysis of the theories on partitioning between the gas and aerosol

particulate phases in the atmosphere. *Atmos. Environ.* 21: 2275–2283.

Pankow, J.F. and Bidleman, T.F. (1992). Interdependence of the slopes and intercepts from log-log correlations of measured gas-particle partitioning and vapor pressure-I. Theory and analysis of available data. *Atmos. Environ.* 26: 1071–1080.

Pankow, J.F. (1994). An absorption model of gas/particle partitioning of organic compounds in the atmosphere. *Atmos. Environ.* 28: 185–188.

Ramirez, N., Cuadras, A., Rovira, E., Marce, R.M. and Borrull, F. (2011). Risk assessment related to atmospheric polycyclic aromatic hydrocarbons in gas and particle phases near industrial sites. *Environ. Health Perspect.* 119: 1110–1116.

Ravindra, K., Sokhi, R. and Van Grieken, R. (2008). Atmospheric polycyclic aromatic hydrocarbons: Source attribution, emission factors and regulation. *Atmos. Environ.* 42: 2895–2921.

Saha, M., Maharana, D., Kurumisawa, R., Takada, H., Yeo, B.G., Rodrigues, A.C., Bhattacharyan, B., Kumata, H., Okuda, T., He, K., Ma, Y., Nakajima, F., Zakaria, M.P., Giang, D.H. and Viet, P.H. (2017). Seasonal trends of atmospheric PAHs in five Asian megacities and source detection using suitable biomarkers. *Aerosol Air Qual. Res.* 17: 2247–2262.

Sharma, H., Jain, V.K. and Khan, Z.H. (2007). Characterization and source identification of polycyclic aromatic hydrocarbons (PAHs) in the urban environment of Delhi. *Chemosphere* 66: 302–310.

Tan, J., Bi, X., Duan, J., Rahn, K., Sheng, G. and Fu, J. (2006). Seasonal variation of particulate polycyclic aromatic hydrocarbons associated with PM_{10} in Guangzhou, China. *Atmos. Res.* 80: 250–262.

Terzi, E. and Samara, C. (2004). Gas-particle partitioning of polycyclic aromatic hydrocarbons in urban, adjacent coastal, and continental background sites of western Greece. *Environ. Sci. Technol.* 38: 4973–4978.

Tobiszewski, M. and Namiesnik, J. (2012). PAH diagnostic ratios for the identification of pollution emission sources. *Environ. Pollut.* 162: 110–119.

Tomaz, S., Shahpoury, P., Jaffrezo, J.L., Lammel, G., Perraudin, E., Villenave, E. and Albinet, A. (2016). One-year study of polycyclic aromatic compounds at an urban site in Grenoble (France): Seasonal variations, gas/particle partitioning and cancer risk estimation. *Sci. Total Environ.* 565: 1071–1083.

Van Drooge, B.L., Fernández, P., Grimalt, J.O., Stuchlík, E., Torres García, C.J. and Cuevas, E. (2010). Atmospheric polycyclic aromatic hydrocarbons in remote European and Atlantic sites located above the boundary mixing layer. *Environ. Sci. Pollut. Res.* 17: 1207–1216.

Wang, W., Simonich, S. L. M., Wang, W., Giri, B., Zhao, J., Xue, M., Cao, J., Lu, X. and Tao, S. (2011). Atmospheric polycyclic aromatic hydrocarbon concentrations and gas/particle partitioning at background, rural village and urban sites in the North China Plain. *Atmos. Res.* 99: 197–206.

Wang, X., Thai, P.K., Li, Y., Li, Q., Wainwright, D., Hawker, D.W. and Mueller, J.F. (2016). Changes in atmospheric concentrations of polycyclic aromatic hydrocarbons and polychlorinated biphenyls between the 1990s and 2010s in an Australian city and the role of bushfires as a source. *Environ. Pollut.* 213: 223–231.

Wang, Z., Na G., Ma, X., Fang, X., Ge, L., Gao, H. and Yao, Z. (2013). Occurrence and gas/particle partitioning of PAHs in the atmosphere from the North Pacific to the Arctic Ocean. *Atmos. Environ.* 77: 640–646.

Wu, S.P., Yang, B.Y, Wang, X.H., Yuan, C.S. and Hong, H.S. (2014). Polycyclic aromatic hydrocarbons in the atmosphere of two subtropical cities in southeast China: Seasonal variation and gas/particle partitioning. *Aerosol Air Qual. Res.* 14: 1232–1246.

Xia, Z., Duan, X., Tao, S., Qiu, W., Liu, D., Wang, Y., Wei, S., Wang, B., Jiang, Q., Lu, B., Song, Y. and Hu, X. (2013). Pollution level, inhalation exposure and lung cancer risk of ambient atmospheric polycyclic aromatic hydrocarbons (PAHs) in Taiyuan, China. *Environ. Pollut.* 173: 150–156.

Yamasaki, H., Kuwata, K. and Miyamoto, H. (1982). Effects of ambient temperature on aspects of airborne polycyclic aromatic hydrocarbons. *Environ. Sci. Technol.* 16: 189–194.

Yang, F., Zhang, Q., Guo, H. and Zhang, S. (2010a). Evaluation of cytotoxicity, genotoxicity and teratogenicity of marine sediments from Qingdao coastal areas using in vitro fish cell assay, comet assay and zebrafish embryo test. *Toxicol. in Vitro* 24: 2003–2011.

Yang, H., Lai, S., Hsieh, L., Hsueh, H. and Chi, T. (2002). Profiles of PAH emission from steel and iron industries. *Chemosphere* 48: 1061–1074.

Yang, T.T, Hsu, C.Y., Chen, Y.C, Young, L.H., Huang, C.H. and Ku, C.H. (2017). Characteristics, sources, and health risks of atmospheric $PM_{2.5}$-bound polycyclic aromatic hydrocarbons in Hsinchu, Taiwan. *Aerosol Air Qual. Res.* 17: 563–573.

Yang, Y., Guo, P., Zhang, Q., Li, D., Zhao, L. and Mu, D. (2010b). Seasonal variation, sources and gas/particle partitioning of polycyclic aromatic hydrocarbons in Guangzhou, China. *Sci. Total Environ.* 408: 2492–2500.

Zhai, Y., Li, P., Zhu, Y., Xu, B., Peng, C., Wang, T., Li, C. and Zeng, G. (2016). Source apportionment coupled with gas/particle partitioning theory and risk assessment of polycyclic aromatic hydrocarbons associated with size-segregated airborne particulate matter. *Water Air Soil Pollut.* 227: 44.

Zhu, Y, Yang, L.X, Yuan, Q., Yan, C., Dong, C., Meng, C.P, Sui, X., Yao, L., Yang, F., Lu, Y.L. and Wang, W.X. (2014). Airborne particulate polycyclic aromatic hydrocarbon (PAH) pollution in a background site in the North China Plain: Concentration, size distribution, toxicity and sources. *Sci. Total Environ.* 466–467: 357–368.

Received for review, January 31, 2018
Revised, March 16, 2018
Accepted, March 17, 2018